ChemPubSoc Europe

DOI: 10.1002/chem.201405991

CHEMISTRY
A European Journal
Full Paper

G-Quadruplexes

Dinuclear Ruthenium(II) Complexes That Induce and Stabilise G-Quadruplex DNA

Li Xu,[a, b] Xiang Chen,[a] Jingheng Wu,[a] Jinquan Wang,[a] Liangnian Ji,[a] and Hui Chao*[a]

Abstract: A series of dinuclear ruthenium(II) complexes were synthesised, and the complexes were determined to be new highly selective compounds for binding to telomeric G-quadruplex DNA. The interactions of these complexes with telomeric G-quadruplex DNA were studied by using circular dichroism (CD) spectroscopy, fluorescence resonance energy transfer (FRET) melting assays, isothermal titration calorimetry (ITC) and molecular modelling. The results showed that the complexes **1**, **2** and **4** induced and stabilised the formation of antiparallel G-quadruplexes of telomeric DNA in the absence of salt or in the presence of 100 mM K^+-containing buffer. Furthermore, complexes **1** and **2** strongly bind to and effectively stabilise the telomeric G-quadruplex structure and have significant selectivity for G-quadruplex over duplex DNA. In comparison, complex **3** had a much lesser effect on the G-quadruplex, suggesting that possession of a suitably sized plane for good π–π stacking with the G-quadruplets is essential for the interaction of the dinuclear ruthenium(II) complexes with the G-quadruplex. Moreover, telomerase inhibition by the four complexes and their cellular effects were studied, and complex **1** was determined to be the most promising inhibitor of both telomerase and HeLa cell proliferation.

Introduction

The DNA G-rich single strand can fold into higher-order structures called G-quadruplexes under appropriate cationic conditions.[1–3] Quadruplexes are present in many biologically significant genomic regions, including telomeres,[4] immunoglobulin switch regions,[5] mutational hot spots and regulatory elements in oncogene promoters,[6–8] and can modulate several biological key processes. For example, G-quadruplexes present in telomeric DNA have been suggested to inhibit telomerase activity (an enzyme that is over-expressed in 85–90% of cancer cells) and to interfere with the biological function of telomere.[9] The G-quadruplexes in many oncogene promoters function as a transcriptional repressor element. Therefore, small molecules that can promote G-quadruplex formation or stabilisation have become an attractive approach towards anticancer drug discovery[.[10–13] However, these G-quadruplex stabilisers show relatively weak selectivity over duplex DNA. Ligand interaction with duplex DNA leads to acute toxicity and drastic side effects in normal tissues.[14] In addition, G-quadruplexes are rich in sequence-dependent structural polymorphisms.[15] Different guanine-rich sequences are well known to fold into different quadruplex conformations in numerous ways. Even the same sequence can fold differently depending on many factors related to the surrounding solution, such as the counterions present (K^+ and Na^+).[16,17] Although telomere sequences can exhibit a range of topologies, conformational selectivity has been only a few considered in almost all of the ligands or complexes recently reported to demonstrate good G-quadruplex affinity and stabilisation ability.[18,19] Furthermore, other authors have suggested that G-quadruplex stabilisers should also be designed to selectively target antiparallel and hybrid-type G-quadruplex folding topologies because the parallel G-quadruplex structure of vertebrate telomeric repeat sequences is not the preferred folding topology under physiological conditions.[17,20] Thus, the improvement of G-quadruplex selectivity is necessary because ligands that bind to specific conformations of human telomeric DNA can lead to the development of disease-specific therapeutic effects and to their utilisation as personal drugs.

Ruthenium(II) complexes have been reported to be G-quadruplex stabilisers[21–25] and probes.[26–29] Ruthenium(II) complexes, especially dinuclear ruthenium(II) complexes, offer substantial advantages over organic compounds,[30–35] other metal complexes (Pt, Ni, etc.)[36–40] and even mononuclear ruthenium(II) complexes,[21,25,28,29] including greater variations in shape, charge and size. By connecting two metal centres into a dinuclear complex, selectivity for G-quadruplex structures can be achieved and the drug tolerance of tumour cells

[a] Dr. L. Xu,[+] X. Chen,[+] J. Wu, J. Wang, Prof. L. Ji, Prof. Dr. H. Chao
MOE Key Laboratory of Bioinorganic
and Synthetic Chemistry
School of Chemistry and Chemical Engineering
Sun Yat-Sen University
Guangzhou 510275 (P.R. China)
E-mail: ceschh@mail.sysu.edu.cn

[b] Dr. L. Xu[+]
School of Chemistry and Chemical Engineering
Guangdong Pharmaceutical University
Zhongshan, 528458 (China)

[+] These authors contributed equally to this work.

Supporting information for this article is available on the WWW under http://dx.doi.org/10.1002/chem.201405991.

to platinum anticancer drugs can be reduced. In addition, two metals are preferred over one because metals incorporated as a structural locus not only restrict the geometry of the planar aromatic core but also serve as a binding element for the substituents of the core.[39] Several recent notable reports have shown that dinuclear ruthenium(II) complexes can induce the formation of and stabilise G-quadruplexes.[21,25] With all of the important influencing factors in mind, we recently synthesised four dinuclear ruthenium(II) complexes (Scheme 1). Surprisingly, some of them can efficiently induce the formation and stabilisation of antiparallel G-quadruplex structures of the human telomeric sequence ($AG_3(T_2AG_3)_3$, HTG22) and can even lead to the conversion of a hybrid G-quadruplex to an antiparallel G-quadruplex. These complexes can also selectively bind and stabilise G-quadruplexes in the presence of excessive duplex DNA. Importantly, the complexes can significantly inhibit telomerase activity and HeLa cell proliferation.

Results and discussion

Synthesis and characterisation

Complexes **1**–**4** (Scheme 1) were prepared by the direct reaction of the ebipcH_2 (2,2′-(9-ethyl-9*H*-carbazole-3,6-diyl)bis-(1*H*-imidazo[4,5-f][1,10]phenanthroline)), mbpibH_2 (1,3-bis(1*H*-imidazo[4,5-f][1,10]phenanthrolin-2-yl)benzene), TpipibH_2 (*N*-(4-(1*H*-imidazo[4,5-f][1,10]phenanthrolin-2-yl)phenyl)-4-(1*H*-imidazo[4,5-f][1,10]phenanthrolin-2-yl)-*N*-phenylaniline) or hbpibH_2 (2,6-bis(1*H*-imidazo[4,5-f][1,10]phenanthrolin-2-yl)-4-methylphenol) ligand with the appropriate molar ratio of the precursor complex, *cis*-[Ru(bpy)$_2$Cl$_2$]·2H$_2$O (bpy = bipyridine), in ethylene glycol; the complexes were obtained in relatively high yields. All of these ruthenium(II) complexes were purified by column chromatography and were characterised by elemental analysis, ^{1}H NMR spectroscopy and ES-MS (see Figures S1–S4 in the Supporting Information). Meanwhile, the four mononuclear complexes were also synthesised (see Figures S5–S12 in the Supporting Information). Because of the very poor solubility of mononuclear ruthenium(II) complexes in aqueous solution, the following experiments were tested only with the dinuclear ruthenium(II) complexes.

Circular dichroism measurements

Circular dichroism (CD) spectroscopy is a conventional method for determining the presence of a G-quadruplex structure and its different folding structures and the effect of complex binding on the quadruplex structures.[41] The interaction of the complexes with telomeric DNA was studied by using this method. Human telomeric DNA can exist as a mixture of antiparallel and parallel G-quadruplex conformations. Previous studies have shown that some G-quadruplex DNA binders can interact with both conformations.[41–43] The CD spectrum of an antiparallel-stranded G-quadruplex exhibits a characteristic positive peak at $\lambda = 295$ nm, a smaller negative peak at $\lambda = 265$ nm and a smaller positive peak at $\lambda = 245$ nm.[44,45] However, the CD spectrum of a parallel-stranded G-quadruplex exhibits a positive peak at $\lambda = 260$ nm and a small negative peak at $\lambda = 240$ nm. In the absence of salt, the CD spectrum of the HTG22 oligonucleotide was partially dissociated to single-stranded molecules with a small negative band centred at $\lambda = 240$ nm, a major positive band at $\lambda = 256$ nm, a minor negative band at $\lambda = 270$ nm and a positive band near $\lambda = 295$ nm (Figure 1 a, black line). Upon the addition of an excess of complex

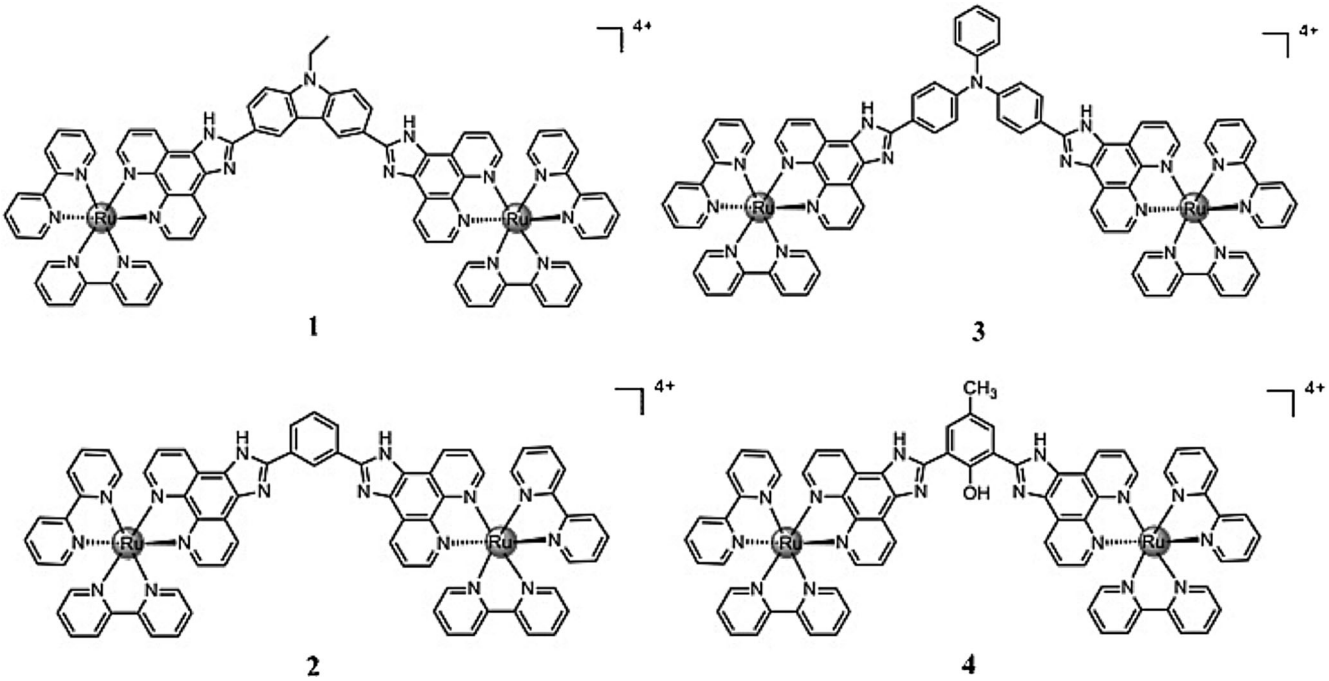

Scheme 1. Chemical structures of the ruthenium(II) complexes **1**–**4**.

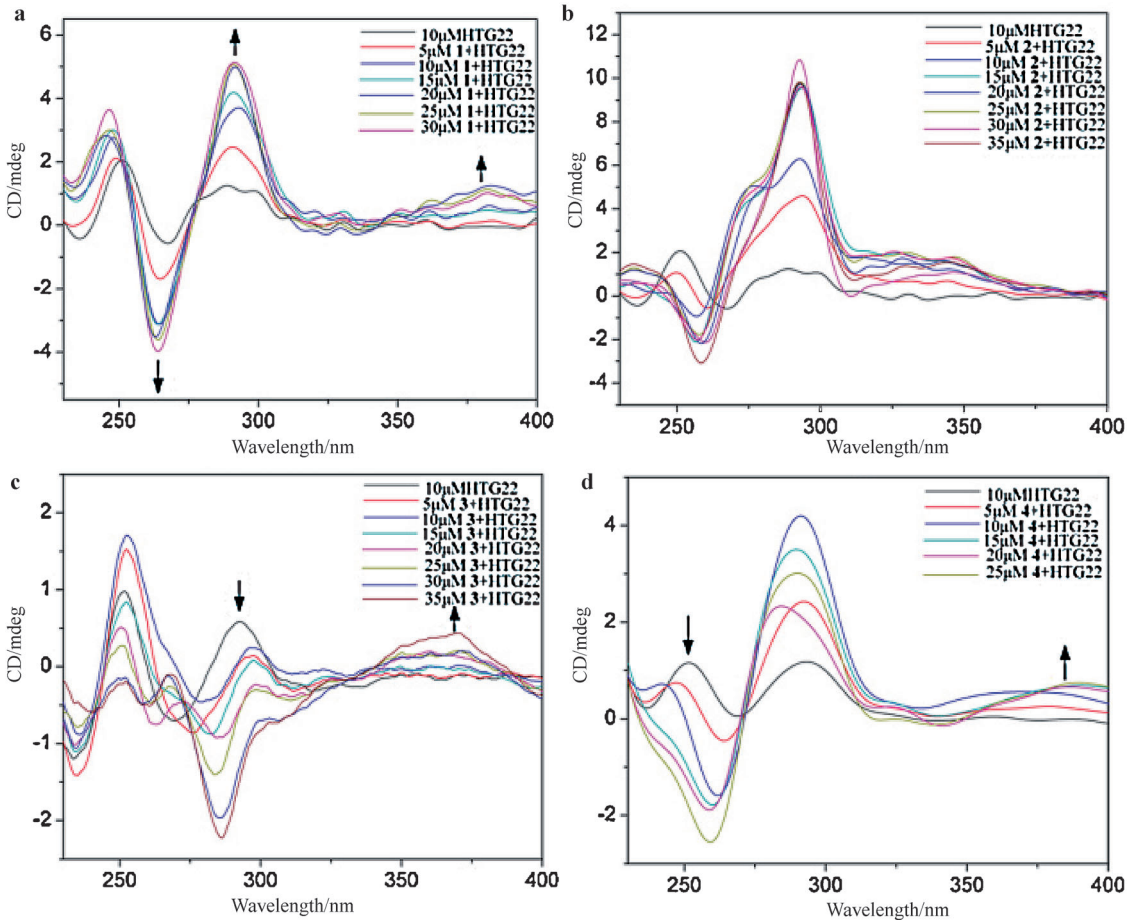

Figure 1. CD spectra of HTG22 (10 μM) induced after the addition of the ruthenium(II) complexes a) **1**, b) **2**, c) **3** and d) **4** at 25 °C in a Tris-HCl buffer (10 mM, pH 7.4).

1 (5 mol equiv) to the HTG22, the CD spectrum changed substantially. The intensity of the band centred at $\lambda = 295$ nm decreased substantially, whereas the small negative band at $\lambda = 240$ nm and the positive band at $\lambda = 256$ nm disappeared, leading to the appearance of a positive band at $\lambda = 245$ nm and a major negative band at $\lambda = 265$ nm (Figure 1a). These changes suggest that complex **1** can induce single-stranded guanine-rich HTG22 DNA to form an antiparallel G-quadruplex structure. The CD spectra of the HTG22 oligonucleotide after the addition of complexes **2** and **4** in the absence of salt were similar to that after the addition of complex **1** (Figures 1b and d). However, the band intensity in the CD spectrum after the addition of complex **2** was weaker than in the spectra after the addition of complexes **1** and **4**. This result indicated that complex **2** was less effective at inducing G-quadruplex formation than with complexes **1** and **4**. Furthermore, upon addition of complex **3** to the HTG22 oligonucleotide, a new and still unclear conformational change was observed in the CD spectrum (Figure 1c).

CD experiments were also measured in solutions containing K^+ and Na^+ to determine whether the compounds could lead to either structural conversion or stabilisation. First, CD titration experiments were performed for the HTG22 oligonucleotide in the presence of 100 mM K^+ buffer. The HTG22 oligonucleotide formed the hybrid-type G-quadruplex structure with a large positive band at $\lambda = 290$ nm, a shoulder at approximately $\lambda = 270$ nm, a small positive band at $\lambda = 250$ nm and a negative band at $\lambda = 235$ nm (see Figure S13 in the Supporting Information, black line).[46] When complex **1** was titrated into the described solution, the CD spectrum significantly changed: the maximum band at $\lambda = 292$ nm increased in intensity and the shoulder at $\lambda = 270$ nm gradually disappeared. In addition, the small positive band at $\lambda = 250$ nm gradually disappeared and led to the appearance of a positive band at $\lambda = 245$ nm and a major negative band at $\lambda = 260$ nm (see Figure S13A in the Supporting Information), indicating that complex **1** can induce the formation of an antiparallel G-quadruplex structure from the hybrid-type G-quadruplex structure (see Figure S13A in the Supporting Information). Similar changes in the CD spectrum were also induced by the addition of complexes **2**–**4** (see Figures S13B–D in the Supporting Information).

Second, we tested the effect of the complexes on the conformation of the HTG22 oligonucleotide formed in a 100 mM NaCl buffer. As shown in Figure S14 in the Supporting Information, in the presence of Na^+ ions and the absence of the ruthenium(II) complexes, the human telomeric sequence adopted an antiparallel conformation.[47] The addition of increasing

amounts of complexes **1**, **3** and **4** to the HTG22 oligonucleotide in a 100 mM Na^+ buffer resulted in no significant changes in the CD spectrum because the G-quadruplex was strongly stabilised by Na^+ (see Figures S14 A, C and D in the Supporting Information). However, the addition of complex **2** resulted in substantial changes, including an increase in the intensity of the positive band at $\lambda = 295$ nm and the disappearance of the small positive band at $\lambda = 240$ nm, which led to the appearance of a positive band at $\lambda = 245$ nm and a shoulder band at $\lambda = 270$ nm (see Figure S14 B in the Supporting Information). These results suggest that complex **2** had the ability to induce the anti-parallel structure of the HTG22 oligonucleotide to form a hybrid-type G-quadruplex structure in the presence of Na^+ ions, whereas complexes **1**, **3** and **4** did not. Overall, the CD experiments clearly demonstrated that complexes **1** and **4** can induce the formation of antiparallel G-quadruplexes with or without the addition of a stabilising salt.

Furthermore, the chiral interferences between the chiral structures of the ruthenium(II) complexes interacting with a G-quadruplex structure have also been considered. We used thermo slide-A-lyzer mini dialysis units with 3500 MWCO to dialysis the complex–DNA mixed solution. Because the molecular weight of the quadruplex–Ru^{II} complex composite structures is larger than 3500, only those chiral ruthenium(II) complexes, which did not bind to the DNA can dialysis out of the dialysis unit. If the complexes have chiral selectivity towards the G-quadruplex structure, this will generate a change of the CD signals, which remained in the dialysis unit. However, no significant CD signal change was observed after 24 h dialysis compared with the samples without dialysis. At the same time, the dialysates outside the dialysis tubes did not exhibit any CD signals. These results demonstrated that there is no obvious difference of binding strength between the different chiral structures of the ruthenium(II) complexes and G-quadruplex (see Figures S15–S17 in the Supporting Information).

Stabilising ability and selectivity studies with Förster resonance energy transfer (FRET)

To investigate the stabilisation effect and the selectivity of the Ru complexes for telomeric G-quadruplex DNA, a FRET melting-point assay was performed to detect the melting temperature. The human telomeric G-quadruplex DNA (F22T) containing fluorophores at both the 5′-end and the 3′-end was used in this assay. The ΔT_m values of the G-quadruplex DNA treated with 1.0 μM solutions of the complexes are shown in Table S1 in the Supporting Information. As shown in Table S1 in the Supporting Information, among all of the complexes, complex **2** had the most distinct ability to stabilise the G-quadruplex DNA, with ΔT_m values of 24 °C in a Na^+ buffer and of 18 °C in a K^+ buffer. The ΔT_m values for complex **1** were similar at approximately 20 °C in a Na^+ buffer and of 12 °C in a K^+ buffer, whereas complexes **3** and **4** showed relatively lower ΔT_m values. The FRET melting data demonstrated that complexes

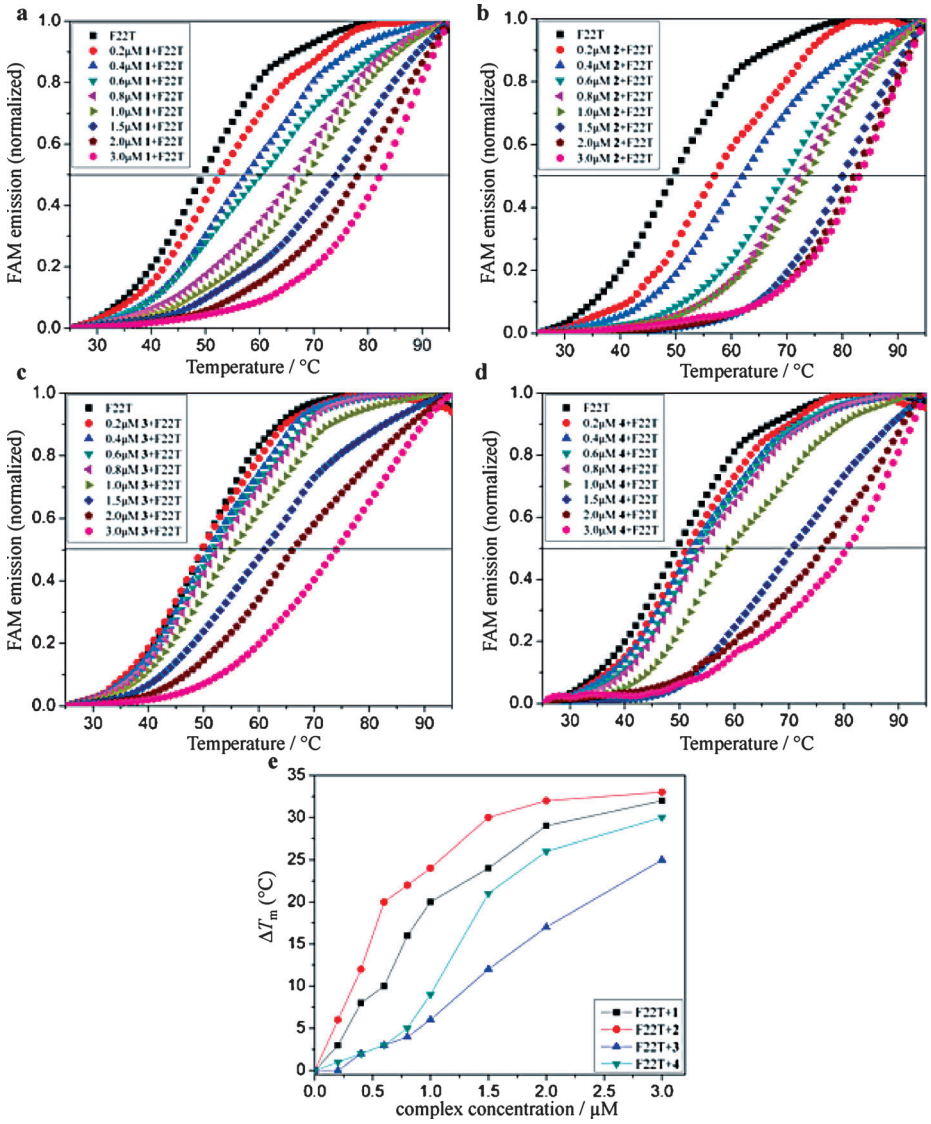

Figure 2. FRET melting profiles of 0.2 μM F22T with the different ruthenium complexes a) **1**, b) **2**, c) **3** and d) **4** in Na^+ buffer. e) Plot of ΔT_m versus the complex concentration.

1 and **2** could effectively stabilise G-quadruplex DNA with much higher ΔT_m values compared to the complexes reported in previous studies. The concentration-dependent melting curves for complexes **1**–**4** in Na^+ and K^+ buffers are shown in Figures 2 and S7 in the Supporting Information, respectively. In the presence of Na^+, the T_m value of the antiparallel G-quadruplex is 50 °C. In the presence of 1 μM of complex **2**, the T_m value increased to 74 °C. This value further increased to 82 °C when the concentration of complex **2** was increased to 3 μM. With the high ionic strength of Na^+ (Figure 2b), the observed ΔT_m value of 32 °C is uncommonly high compared to those reported in previous studies.[33,36,40] In the presence of K^+, we observed a similar phenomenon, but with lower ΔT_m values. For example, the T_m value of the hybrid G-quadruplex in the presence of K^+ is 60 °C; however, in the presence of 1 μM of complex **2**, the T_m value increases by 18 °C (to 78 °C). After the addition of 3 μM of complex **2**, a remarkable melting temperature increase of 24 °C was observed (see Figure S18B in the Supporting Information). Although the ΔT_m values observed for complex **1** were smaller than those for complex **2** in both Na^+ (Figure 2a) and K^+ (see Figure S18A in the Supporting Information) buffers, all of the results suggest that complexes **1** and **2** are suitable G-quadruplex stabilisers. FRET melting experiments were also used to examine the binding selectivity of the complexes on a G-quadruplex over duplex DNA. The DNA competition FRET melting assay was performed to show the ΔT_m change for ruthenium(II) complex concentrations of 0.5 μM, 1.0 μM and 2.0 μM with 200 nM F22T through the addition of various concentrations of the double-stranded DNA ds26. The results of the melting-point change of 1.0 μM ruthenium(II) complexes induced by the addition of ds26 in Na^+ or K^+ buffers are shown in Figure 3 and Figure S19 in the Supporting Information, respectively. The ΔT_m values for complex **1**, **2** and **4** did not significantly decrease, particularly in the Na^+ buffer, despite the presence of ds26 at a concentration

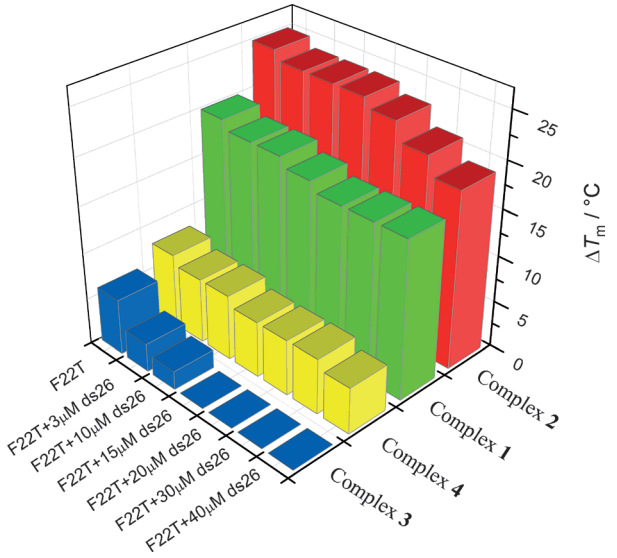

Figure 3. ΔT_m change of F22T under different concentrations of double-stranded DNA ds26 in Na^+ buffer treated with 1 μM of the different Ru complexes.

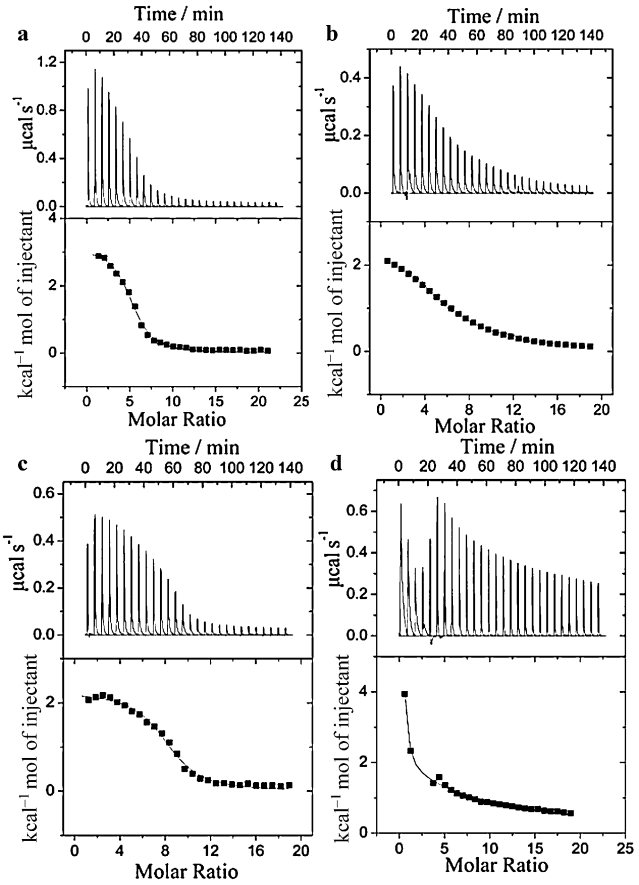

Figure 4. ITC data for the binding of complexes a) **1**, b) **2**, c) **3** and d) **4** to the human telomeric G-quadruplex. The data were obtained in a buffer that consisted of 100 mM NaCl, 10 mM NaH_2PO_4/Na_2HPO_4 and 1 mM Na_2EDTA (EDTA = ethylenediaminetetraacetic acid) (pH 7.0) at 25 °C The binding parameters of complexes **1**–**4** were obtained through analysis of the ITC profiles.

200 times that of F22T. These results indicate that the ruthenium(II) complexes can specifically stabilise the G-quadruplex structure with affecting duplex DNA.

Binding affinity studies with isothermal titration calorimetry (ITC)

To assess the binding affinity and thermodynamic properties of the interaction between the complexes and the G-quadruplexes, we used ITC to determine the chemical thermodynamics, binding constants (K_b) and number of binding sites (n). Representative ITC curves for the binding of complexes **1**–**4** to the HTG22 G-quadruplex DNA at 298 K in a Na^+-containing solution are shown in Figure 4. The thermodynamic parameters for the binding of the four complexes to quadruplex DNA are summarised in Table S2 in the Supporting Information. The binding constants of complexes **1**, **2** and **4** are approximately twice that of complex **3**. These data demonstrate the importance of the intercalating chromophores because complexes **1**–**4** have identical ancillary ligands.

The human telomeric G-quadruplex binding stoichiometry with quadruplex DNA was investigated through luminescence-

based Job plots (see Figure S20 in the Supporting Information). Three major inflection points for three complexes were observed at $x=0.52$ for complex **1**, $x=0.57$ for complex **2** and $x=0.46$ for complex **3**. These data are consistent with a 1:1 [quadruplex]/[complex] binding mode. However, the intersection of the fit lines in the Job plot for human telomeric G-quadruplex with complex **4** is approximately 0.69. This value corresponds to a [complex]/[G-quadruplex] stoichiometric ratio of 2:1. These results are consistent with the results obtained from the ITC study.

Polymerase chain reaction (PCR)-stop assay

To demonstrate that the ruthenium(II) complexes can induce G-quadruplex formation from telomeric DNA, a PCR-stop assay was performed. The PCR-stop assay is an effective method to ascertain whether the complexes bind to the test oligomer, that is, HTG22, and induce its transformation into a G-quadruplex structure.[48] In the lane in which G-quadruplex stabilisers were absent, sequences of HTG22 and its corresponding complementary sequence (HTG22rev) will, under the function of Taq DNA polymerase, hybridise to a final double-stranded DNA PCR product that can be observed as a clear band in both lanes with 0 μM ruthenium(II) complexes. However, in the presence of the four ruthenium(II) complexes, the template sequence HTG22 formed a G-quadruplex structure induced by the ruthenium complexes that the Taq DNA polymerase cannot elongate into a double-stranded structure; thus, the PCR reaction is blocked. The greater the concentration of the ruthenium(II) complex is, the smaller is the amount of final product that can be detected.[19] As the ruthenium(II) complex binds to all of the template sequence HTG22, the band of the PCR product will completely disappear. Figure 5 illustrates the disappearance of the final PCR product under increasing concentrations of the complexes.

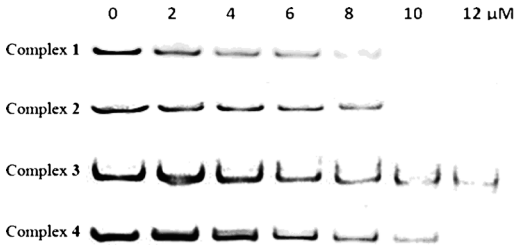

Figure 5. Effects of ruthenium(II) complexes **1**–**4** on the hybridisation of HTG22 in the PCR-stop assay.

The inhibitory effects of all four of the complexes are concentration dependent. Complex **1** exhibited a better G-quadruplex stabilisation activity with complete inhibition of HTG22 at a complex concentration of approximately 10 μM. The same effect of complexes **2** and **4** was observed at approximately 12 μM, whereas the band was still slightly detected in the case of complex **3**, even at a complex concentration of 12 μM. Complexes that exhibit better inhibition of the amplification in HTG22 generally possess a greater G-quadruplex structure-stabilising ability. Meanwhile, the binding selectivity between the HTG22 G-quadruplex and other representative G-quadruplexes in gene promoters, such as c-myc, bcl-2 and c-kit2, has also been tested by using the PCR-stop assay. Experimental results demonstrate that none of these four complexes can significantly inhibit the PCR amplification by interacting with the c-myc, bcl-2 or c-kit2 gene promoters sequence at 14 μM whereas the highest concentration that can inhibit the amplification in the HTG22 sequence is only 12 μM (see Figure S21 in the Supporting Information).

Telomere repeat amplification protocol (TRAP) assay

The complexes synthesised herein were designed to restrain the activity of telomerase. The TRAP assay is a general and reliable method for evaluating the inhibitory properties of small molecules against telomerase in vitro. In previous studies, complexes with a high binding affinity and stabilising ability for telomeric G-quadruplexes were suggested to exhibit inhibitory effects on telomerase.[49] After the complex binds to the telomeric sequence and induces its structural transformation into a G-quadruplex, the geometrical conformation of the telomeric DNA is altered such that its telomerase binding site is lost. The immediate consequence is telomerase inactivity. The intensity of the DNA ladder will reflect the activity of telomerase. To make the experiment more rigorous, we performed a positive control by using the same process used for the other test samples but without the addition of any complexes. In addition, a negative control was performed by using the same process used for the positive control but without the addition of cell extracts. These controls ensure that the DNA ladder is generated by telomerase. The internal control (IC) bands were generated by the sequence that cannot transform into a G-quadruplex; thus, their steady appearance will help to ensure that other factors do not block the PCR during the process. As shown in Figure 6, the number of bands clearly decreased with increasing concentrations of the complexes, showing that the in vitro inhibitory effects of the four complexes toward telomerase are concentration dependent. Complexes **1**, **2** and **4** exhibit a remarkably high inhibitory effect on telomerase at only nanomolar levels. Complex **1**, in particular, causes the DNA ladder to completely disappear at an encouraging concentration of approximately 200 nM. Although complex **3** exhibits less inhibitory activity toward telomerase than the other three complexes, its inhibition concentration of 2 μM still makes it one of the best telomerase inhibitors. Compared with previously reported G-quadruplex ligands,[24,50] all four complexes synthesised herein exhibit an extraordinarily high inhibition activity of telomerase in vitro, which indicates that they are promising potential human telomerase inhibitors.

Short-term cell viability

All of the above results indicate that the four complexes can induce the formation of telomere sequence DNA into anti-par-

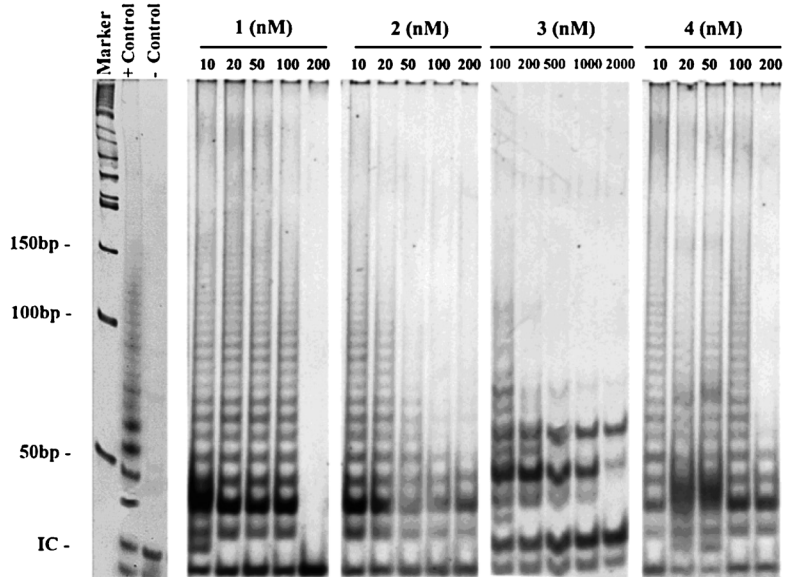

Figure 6. Inhibition of telomerase activity by complexes **1**–**4**. A positive control (+) was performed with telomerase but without ligand. A negative control (−) was performed without either telomerase or ligand. The ladder shows the product of telomerase elongation. The lower band is an internal control primer (IC).

liferation experiment. Figure 7 shows the cell viability (relative to control) as a function of the concentration of the four complexes after incubation for 72 h. All four ruthenium complexes showed mild cytotoxicity compared to cisplatin in the short-term assay. The IC_{50} values of the four complexes **1**–**4** are 33.1, 38.5, 54.2 and 40.8 μM, respectively, whereas that for cisplatin is (8.3 ± 1.4) μM. In addition, the four complexes at concentrations less than 3.13 μM showed no cytotoxicity toward HeLa cells, indicating that concentrations less than this value could be used in the long-term proliferation experiments.

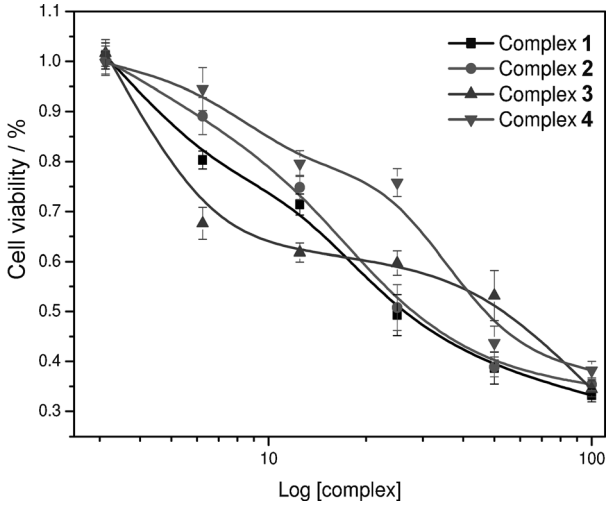

Figure 7. Effect of the ruthenium(II) complexes **1**–**4** on HeLa cell viability. HeLa cells were treated with various concentrations of the ruthenium(II) complexes (3.13–100 μM) for 72 h.

allel structures with high selectivity, leading to high telomerase inhibition in the cell-free system. These results thus encouraged us to discover the function of these four complexes in the cell. Inhibition of telomerase is well known to shorten the telomere. Thus, cell apoptosis will not immediately occur; the cells will enter programmed cell death until the telomere is reduced to a certain point after several cell divisions.[51] On the basis of these considerations, complexes that can become potential telomerase inhibitors must not kill cells immediately. Therefore, short-term cell viability assays will provide a specific concentration that will not influence cell growth with an acute toxicity, which is necessary for the subsequent long-term pro-

Long-term proliferation experiments

As a consequence of telomerase inhibition, telomere sequence elongation will be blocked. A large amount of evidence suggests that a dysfunctional telomere could activate p53 to initiate cellular senescence or apoptosis.[52,53] Because telomere shortening accompanies cell division, this effect will only be observed after several cycles of cell division. Thus, long-term experiments must be performed to eliminate the effects of acute cytotoxicity or other nonspecific events. Therefore, subcytotoxic concentrations (2.5 μM, far below the IC_{50} value) of the complexes were evaluated in HeLa cells during long-term exposure. Figure 8 shows the change in the CI, representing cell growth. At the very beginning, cells that were and were not treated with complexes could not be readily distinguished, indicating that the complexes had no obvious short-term cytotoxic effects. After three days, all of the cells exposed to the complexes were delayed in entering the log phase and the cell number slowly decreased, indicating that the cell activity was reduced. The growth condition of the cells exposed to complexes **1** and **2** was inferior to that of the cells exposed to complexes **3** and **4**. All of these results indicate that the cells were led to apoptosis in the long-term experiments by the four complexes. Furthermore, the complexes showing stronger telomerase inhibition ability in the TRAP assay also exhibited more efficient cell inhibition in the long-term proliferation experiments. Combined with the TRAP assay results, we believe that the long-term cell death caused by the four complexes is a result of the inhibition of telomerase, which leads to telomere-length shortening. Previously reported efficient telomeric G-quadruplex ligands and telomerase inhibitors exhibiting the same experimental results[54] and phenomena support the findings that these four complexes are significant telomerase inhibitors.

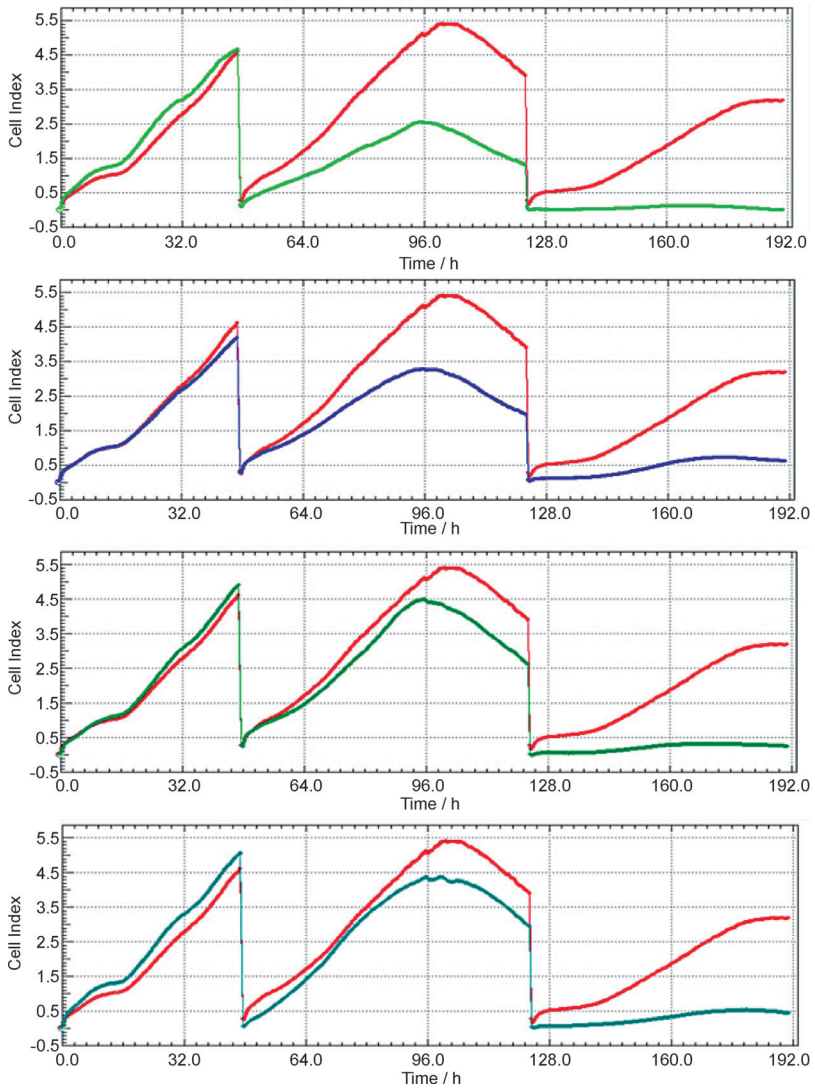

Figure 8. Long-term growth curves of HeLa cells treated with complexes **1** (bright green), **2** (blue), **3** (dark green) and **4** (cyan). The red curve represents control cells not exposed to the complexes.

Molecular docking and MM/GBSA calculations

Molecular docking experiments were performed to elucidate different interactions between the ligands and HTG DNA.[55] The three forms of the complexes, that is, the (Δ,Δ), (Δ,Λ) and (Λ,Λ) form were introduced in the docking analysis. The results showed that these compounds share very similar binding sites (see Figures S22 and S23 in the Supporting Information). For complex **4**, which binds with the DNA as a ratio of 2:1, we presented a binding model including nonspecific binding together with intercalation presented in Figure 9 (by using the (Λ,Λ) form, the same as follows) because there is no evident supporting that covalent bonding is involved between complex **4** and the G-quadruplex. When the nonspecific binding was formed, the complexes inserted into one of the DNA grooves with the planar aromatic ring groups spanning the nucleotides (Figure 9). The intercalation between the ligands and the HTG DNA in an ionic solution containing K^+ ions is shown in Figure 10. As shown in Figure 10, The external-stacking binding mode can easily be found in the binding of K^+-assembled HTG DNA for the base pairs that are exposed to the solvent. Meanwhile, for an ionic solution containing Na^+ ions, the ruthenium(II) complex is stacked on the G-quadruplex and its phenanthroline nitrogen atoms overlap the negative electrostatic potential provided by the polarised carbonyl centre (Figure 9). It clearly shows the importance of π–π interactions, where the central aromatic rings in the ruthenium(II) complex stack onto the surface of the guanines. To further investigate these possible binding modes and to achieve more reliable information, molecular dynamics (MD) simulations and MM/GBSA calculations were carried out. As summarised in Table 1, similar binding free energies (ΔG_{bind}) values were obtained for external stacking. Relatively, due to the larger contact surfaces, stronger ligand/DNA interactions (lower ΔG_{bind} values) were observed for the intercalation binding mode, especially in the cases of complex **1**. Results are in excellent agreement with those related to the stabilising ability of the FRET experiments and the thermodynamic parameters (see Table S2 in the Supporting Information) obtained by using ITC, which indicated that complex **1** exhibits remarkable stabilising abilities, whereas complex **3** shows the worst. Furthermore, the last MD snapshot presented in Figure 11 clearly shows that complexes **1**, **2** and **4** stabilises

Table 1. Calculated binding free energies and their components for the binding of the dinuclear ruthenium(II) complexes to Na^+- (PDB 143D)/K^+ (PDB 1KF1)-assembled human telomeric G-quadruplex DNA (in [kcal mol^{-1}]).

PDB	Binding mode	Complex	ΔG_{ele}	ΔE_{vdW}	$\Delta G_{solv\text{-}np}$	ΔG_{bind}
143D	intercalation	**1**	31.30	−107.35	−8.93	−84.98
		2	30.12	−102.87	−8.97	−81.72
		3	16.06	−69.96	−6.89	−60.79
		4	35.21	−111.08	−9.08	−84.95
1KF1	external stacking	**1**	7.10	−52.60	−5.43	−50.93
		2	9.05	−60.01	−6.01	−56.95
		3	5.78	−50.59	−5.26	−50.06
		4	5.99	−48.90	−5.12	−48.03

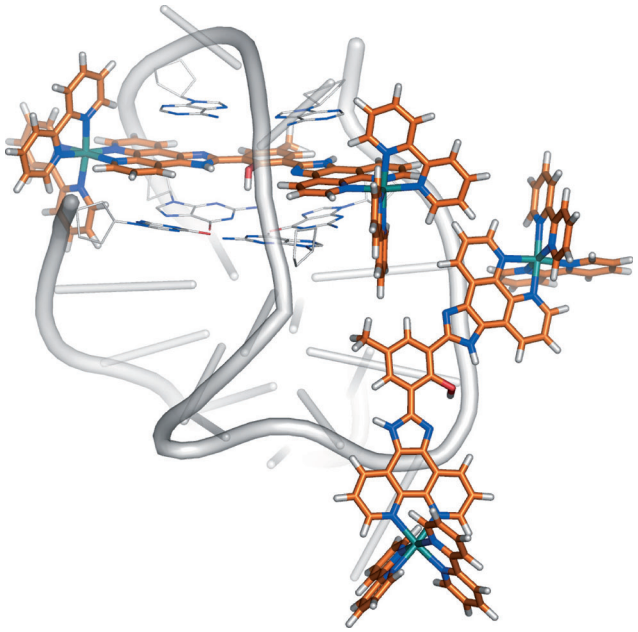

Figure 9. External stacking binding mode of complex **4** and the Na^+-assembled HTG DNA (PDB ID: 143D).

Conclusion

In summary, four ruthenium(II) complexes have been synthesised and characterised. The binding behaviours of the ruthenium(II) complexes towards G-quadruplex DNA were examined by CD spectroscopy and FRET melting assays. These experiments showed that complexes **1**, **2** and **4** can induce high stabilisation of the human telomeric G-quadruplex and possess an extraordinarily high selectivity for the G-quadruplex versus duplex DNA. To examine the abilities of the complexes to bind strongly to telomeric quadruplex DNA and to inhibit cancer proliferation, we also performed TRAP assay and in vitro cytotoxicity studies of the four complexes. The results indicated that complex **1** is a potent inhibitor of telomerase and HeLa cell proliferation. The results also indicated that a dinuclear complex has a higher solubility in aqueous solution and that its geometry structure leads to a better selectivity to G-quadruplex over duplex DNA than the traditional mononuclear complex. In addition, we also achieve some certain results of the structure–function relationship between the main ligands of the metal complex and the G-quadruplex DNA. These results will be valuable for designing more potent and selective telomeric G-quadruplex-interactive compounds.

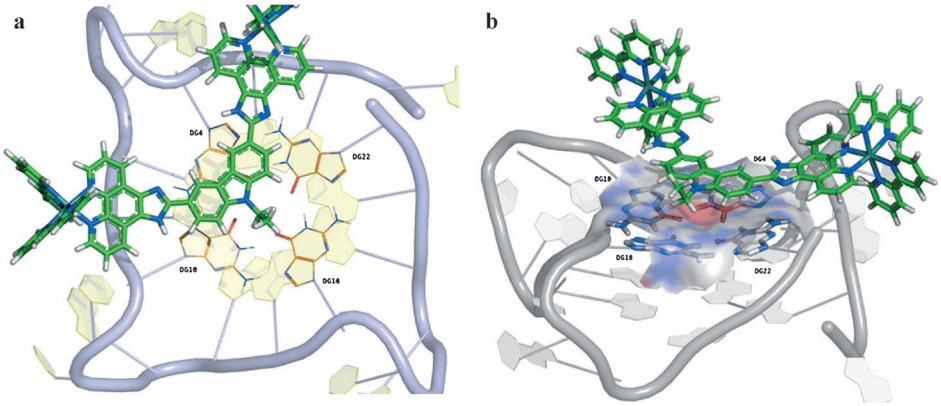

Figure 10. External stacking binding mode of complex **1** and the K^+-assembled HTG DNA (PDB ID: 1 KF1). a) Platform and b) side elevation, red stands for negative-charged regions, blue stands for positive-charged regions.

the DNA strands by spanning over the G-quadruplex. Even without the central ions, the conformations of the planar G-quadruplets did not change obviously in the stabilisation of these two ligands. However, the DNA chain bound to the less effective complex **3** was not stabilised, indicating that the G-quadruplets did not maintain their original planar conformation and the bases scattered after 4.2 ns of MD equilibration. According to the component analysis of the ΔG_{bind} values (Table 1), the primary contributors to the binding free energies were van der Waals energies. Therefore, the lower stabilising ability of complex **3** can be explained by its non-planar conformation, which was disadvantageous toward the stacking of complex **3** on the planar G-quadruplets.

Experimental Section

Materials: The human telomeric sequence d[$(TTAGGG)_n$] (HTG22) DNA, DNA F22T (5′-FAM-d(AG_3[$TTAGGG]_3$)-TAMRA-3′) (FAM06-carboxy fluorescein, TAMRA = 6-carboxytetramethylrhodamine), DNA ds26 (5′-CAATCGGATCGAATTCGAT-CCGATTG-3′), the oligomers HTG22 (5′-AGGGTTAGGGTTAGGGTTAGGG) and the corresponding complementary sequences HTG22rev (5′-ATACGCTTCTCGTCCCTAACCC), the oligomers c-myc (5′-TGGGGAGGGTGGGGAGGGTGGGGAAGG) and the corresponding complementary sequences Rev c-myc (5′-GATCTTCTTCGTCCTTCCCCA), the oligomers bcl-2 (5′-CGGGCGCGGGAGGAAGGGGGCGGGAGC) and the corresponding complementary sequences Rev bcl-2 (5′-ATCGATCGCTTCT-CGTGCTCCCGCCC), the oligomers c-kit2 (5′-CGGGCGGGCGCGAGGG-AGGGG) and the corresponding complementary sequences Rev c-kit2 (5′-TATATATATACCCCTCCCT) were obtained from Sangon Biological Engineering Technology & Services Co., Ltd. (Shanghai, China). Acrylamide (molecular biology grade) and ethidium bromide were purchased from Sigma (USA). HeLa (cervical) cell lines were purchased from American Type Culture Collection. Other materials were commercially available and of reagent grade. Doubly distilled or DEPC-treated water (DEPC = diethylpyrocarbonate) were used to prepare the buffers. A solution of HTG22 in the buffer gave a ratio of UV absorbance at $\lambda = 260$ and 280 nm of approximately (1.8–1.9):1, indicating that the DNA was sufficiently free of protein.[53] The DNA concentration per nucleo-

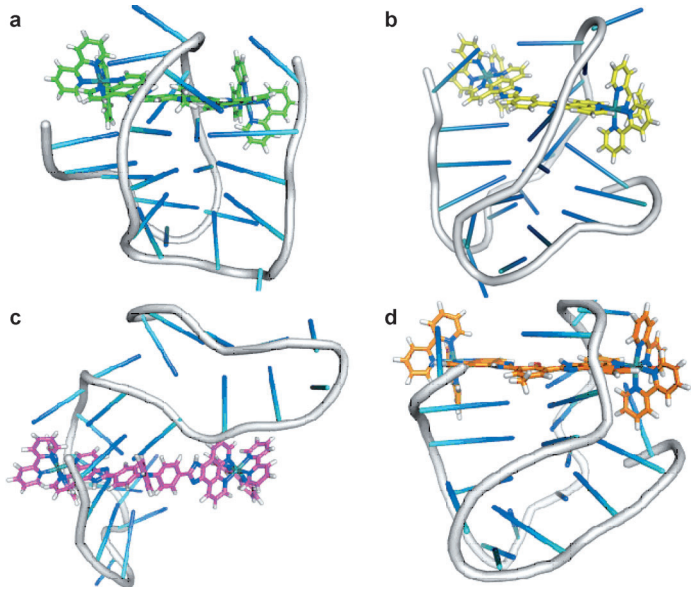

Figure 11. The last snapshots of 4.2 ns of MD equilibration for the Na^+-assembled HTG DNA and the dinuclear ruthenium(II) complexes a) **1**, b) **2**, c) **3** and d) **4**.

tide was determined by absorption spectroscopy by using the molar absorptivity (2.285×10^5 mol(quadruplex)$^{-1}$ m^{3}cm^{-1}) at $\lambda=$ 260 nm.[15] The buffers were prepared as follows: 1) 10 mM Tris-HCl, pH 7.4; 2) 100 mM NaCl, 10 mM NaH_2PO_4/Na_2HPO_4 and 1 mM Na_2EDTA (pH 7.0) and 3) 100 mM KCl, 10 mM KH_2PO_4/K_2HPO_4 and 1 mM K_2EDTA (pH 7.0).

Physical measurements: Microanalysis (C, H and N) was performed by using a Vario EL elemental analyser. Fast atomic bombardment mass spectra (FAB-MS) were detected on a VG ZAB-HS spectrometer in a 3-nitrobenzyl alcohol matrix. Electrospray mass spectra (ES-MS) were recorded on an LCQ system (Finnigan MAT, USA). ^{1}H NMR spectra were recorded at room temperature on a Varian INOVA-500 spectrometer by using $(CD_3)_2SO$ as the solvent and $SiMe_4$ as an internal standard. All chemical shifts are reported relative to TMS. CD spectra were recorded at room temperature on a JASCO J-810 spectropolarimeter in a cylindrical quartz cell with a path length of 0.2 cm.

Synthesis of ligands and the Ru^{II} complexes: The compounds $[(bpy)_2Ru(ebipcH_2)Ru(bpy)_2](ClO_4)_4$ (**1**),[56] $[(bpy)_2Ru(mbpibH_2)Ru(bpy)_2](ClO_4)_4$ (**2**),[57] 1,10-phenanthroline-5,6-dione,[58] *cis*-$[Ru(bpy)_2Cl_2]\cdot2H_2O$[59] and 4,4′-(phenylazanediyl)-dibenzaldehyde[60] were synthesised according to literature methods. All other reagents were obtained commercially and used as received.

Synthesis of the TpipibH$_2$ ligand: A mixture of 4,4′-(phenylazanediyl)dibenzaldehyde (0.45 g, 1.5 mmol), 1,10-phenanthroline-5,6-dione (0.63 g, 3 mmol), ammonium acetate (4.62 g, 60 mmol) and glacial acetic acid (50 cm^3) was heated to reflux with stirring for 2 h. The cooled solution was then diluted with water and neutralised with concentrated aqueous ammonia. The precipitate was collected and purified by column chromatography on silica gel (60–100 mesh) with ethanol as the eluent to give the compound as a yellow powder. Yield: 0.59 g, 58%; FAB-MS: *m/z*: 683 [*M*+1]; elemental analysis calcd (%) for $C_{44}H_{27}N_9$: C 77.52, H 3.99, N 18.49; found: C 77.02, H 4.08, N 18.35.

Synthesis of the hbpibH$_2$ ligand: This ligand was synthesised by a method identical to that described for TpipibH$_2$, except that 2-hydroxy-5-methylisophthalaldehydein was substituted for 4,4′-(phenylazanediyl)-dibenzaldehyde. Yield: 0.49 g, 60%; FAB-MS: *m/z*: 545 [*M*+1]; elemental analysis calcd (%) for $C_{33}H_{20}N_8O$: C 72.78, H 3.70, N 20.58; found: C 72.75, H 3.72, N 20.62.

Synthesis of $[(bpy)_2Ru(TpipibH_2)Ru(bpy)_2](ClO_4)_4$ (3): A mixture of *cis*-$[Ru(bpy)_2Cl_2]\cdot2H_2O$ (0.31 g, 0.58 mmol) and TpipibH$_2$ (0.20 g, 0.29 mmol) in ethylene glycol (40 cm^3) was heated to reflux under argon for 12 h to give a clear red solution. After the solution was cooled, a red precipitate was obtained by dropwise addition of a saturated aqueous solution of $NaClO_4$. The crude product was purified by column chromatography on neutral alumina with acetonitrile as the eluent. The red band was collected and the solvent was removed under reduced pressure to give a red powder. Yield: 0.39 g, 70%; ^{1}H NMR (500 MHz, [D$_6$]DMSO): $\delta=10.07$ (d, $J=8$ Hz, 2H), 9.03 (d, $J=8$ Hz, 2H), 8.89 (d, $J=8$ Hz, 2H), 8.85 (d, $J=8$ Hz, 4H), 8.82 (d, $J=8$ Hz, 4H), 8.40 (d, $J=7$ Hz, 2H), 8.30 (d, $J=8$ Hz, 2H), 8.25 (t, $J=8$ Hz, 2H), 8.21 (t, $J=5.5$ Hz, 4H), 8.15 (t, $J=5$ Hz, 4H), 8.11 (t, $J=3$ Hz, 2H), 7.92 (d, $J=8$ Hz, 2H), 7.86 (d, $J=5$ Hz, 4H), 7.84–7.79 (m, 4H), 7.65–7.56 (m, 7H), 7.45–7.35 (m, 6H), 7.27–7.18 ppm (m, 4H); ES-MS (CH_3CN): *m/z*: 803.4 $[M-3ClO_4-H]^{2+}$, 753.6 $[M-4ClO_4-2H]^{2+}$, 535.8 $[M-3ClO_4]^{3+}$, 502.3 $[M-4ClO_4-H]^{3+}$, 376.8 $[M-4ClO_4]^{4+}$; elemental analysis calcd (%) for $C_{84}H_{59}N_{17}Cl_4O_{16}Ru_2$: C 52.92, H 3.12, N 12.49; found: C 53.12, H 3.04, N 12.38.

Synthesis of $[(bpy)_2Ru(hbpibH_2)Ru(bpy)_2](ClO_4)_4$ (4): This complex was synthesised by a method identical to that described for the preparation of $[(bpy)_2Ru(TpipibH_2)Ru(bpy)_2](ClO_4)_4$, except that hbpibH$_2$ (0.16 g, 0.29 mmol) was used instead of TpipibH$_2$. Yield: 0.33 g, 65%; ^{1}H NMR (500 MHz, [D$_6$]DMSO): $\delta=9.78$ (br s, 1H), 9.18 (d, $J=8$ Hz, 4H), 8.87 (d, $J=8$ Hz, 4H), 8.83 (d, $J=8$ Hz, 4H), 8.26 (s, 2H), 8.22 (dt, $J_1=J_2=8$ Hz, 4H), 8.11 (dt, $J_1=J_2=8$ Hz, 4H), 8.00 (d, $J=5$ Hz, 4H), 7.91–7.84 (m, 8H), 7.63 (d, $J=5.5$ Hz, 4H), 7.60 (dt, $J_1=J_2=5$ Hz, 4H), 7.36 (dt, $J_1=J_2=7$ Hz, 4H), 2.50 ppm (s, 3H); ES-MS (CH_3CN) *m/z*: 734.1 $[M-3ClO_4-H]^{2+}$, 685.1 $[M-4ClO_4-2H]^{2+}$, 457.6 $[M-4ClO_4-H]^{3+}$, 342.4 $[M-4ClO_4]^{4+}$; elemental analysis calcd (%) for $C_{73}H_{52}N_{16}Cl_4O_{17}Ru_2$: C 49.56, H 2.96, N 12.67; found: C 49.43, H 3.01, N 12.56.

Circular dichroism measurements: CD experiments to investigate the interaction of the complexes with the HTG22 G-quadruplex were recorded on a JASCO J-810 spectropolarimeter at room temperature by using a quartz cell with a path length of 0.2 cm. CD spectra were collected from 200 to 400 nm with a scanning speed of 500 nm min^{-1}. The bandwidth was 8.53 nm, the response time was 0.5 s and each sample was scanned three times to obtain an average measurement. The solutions of HTG22 (10 μM) with various concentrations of the Ru^{II} complexes (0–5 mol equiv) were prepared in different buffers and stored at 4 °C overnight before measurement.

FRET assay: A FRET melting point assay was used to investigate the ability of the Ru^{II} complexes to stabilise the G-quadruplex. The fluorescent-labelled oligonucleotide F22T was prepared as a 100 μM stock solution in buffers B and C and annealed at 90 °C for 5 min. After being heated, the annealed sample was slowly cooled to room temperature. Fluorescence melting curves were measured on a Bio-Rad IQ 5 real-time PCR detection system by using a total reaction volume of 25 μL, 500 nM of labelled oligonucleotide and different concentrations of the ruthenium(II) complexes. Fluorescence readings with excitation at $\lambda=470$ nm and detection at $\lambda=530$ nm were taken at intervals of 1 °C in the tem-

perature range of 25 to 95 °C. Each temperature was maintained for 30 s before the reading was taken to ensure that the sample had reached equilibrium. A DNA competition FRET melting assay was performed to explore the selectivity of the Ru^{II} complexes between duplex DNA and G-quadruplex DNA. All of the conditions of the reaction system were similar to those used in the FRET melting point assay, except that different concentrations of duplex DNA ds26 were added.[61,62]

Isothermal titration calorimetry (ITC): Calorimetric experiments were performed by using a high-sensitivity isothermal titration calorimeter (VP-ITC, MicroCal, Inc., Northampton, MA, USA). All of the solutions were thoroughly degassed before use by being stirred under vacuum for 0.5 h in buffer B at 25 °C. The human telomeric G-quadruplex DNA solutions for use in the ITC experiments were prepared by dilution of the stock DNA solution with the dialysis buffer. The ruthenium complexes were dissolved in buffer B. The sample cell was loaded with 1.43 mL of G-quadruplex DNA solution, and the reference cell was loaded with doubly distilled water. For a typical titration, 10 μL of the complex solution were injected into a sample cell of the DNA solution at 300 s intervals with a stirring speed of 370 rpm. The heat output per injection was obtained through integration and was corrected by subtraction of the dilution heat, which was determined in parallel experiments by using an injection of the same concentrations of complex into the buffer solution. The corrected binding isotherms were fitted by using the Origin 7.0 software to obtain the K_b value, the number of binding sites (n), the enthalpy change (ΔH) and the entropy change (ΔS).

Continuous *variation* analysis: Continuous variation analysis was performed according to a previously reported literature procedure.[63] Stock solutions of 100 μM complex were prepared. The human telomeric G-quadruplex DNA solution was prepared to match the concentration of the stock solutions in buffer B. The concentrations of both the complex and the DNA were varied, whereas the sum of the reactant concentrations was kept constant at 10 μM. In the sample solutions, the mole fraction, χ, of the complex was varied from 0 to 1.0 in ratio steps of 0.1. The fluorescence intensities of these mixtures were measured at 25 °C. The fluorescence intensity was plotted as a function of the mole fraction of the complex to generate a Job plot. Linear regression analysis of the data was performed by using the Origin 7.0 software.

PCR-stop assay: The PCR-stop assay was used to investigate the effect of amplification inhibition induced by the Ru^{II} complexes. In the absence of a G-quadruplex stabiliser, the human telomere sequence (HTG22) can amplify under the use of Taq DNA polymerase and hybridise a final double-stranded DNA PCR product with its corresponding complementary sequence, HTG22rev. After the Ru^{II} complexes bind to HTG22 and stabilise it by transforming it into a more stable formation, such as a G-quadruplex structure, the PCR reaction will be restrained by this transformation. The increase in the concentration of G-quadruplex stabilisers will decrease the yield of the final PCR product. The PCR-stop assay was performed by using a modified version of a protocol reported in a previous study.[64] Four oligomers were used in the current study: HTG22 (5′-AGGGTTAGGGTTAGGGTTAGGG), c-myc (5′-TGGGGAGGGTGGGGAGGG-TGGGGAAGG), bcl-2 (5′- CGGGCGCGGGAGGAAGGGGGCGGGAGC), c-kit2 (5′- CGGGCGGGCGCGAGGGAGGGG) and the corresponding complementary sequence HTG22rev (5′-ATACGCTTCTCGTCCCTAACCC), Rev c-myc (5′-GATCTTCTTCGTCCTTCCCCA), Rev bcl-2 (5′- ATCGATCGCTTCTCGTGCT-CCCGCCC) and Rev c-kit2 (5′- TATATATATACCCCTCCCT). The reactions were performed in a 1×PCR buffer containing 600 nmol of HTG22 and 1000 nM HTG22rev, 0.16 mM dNTPs and 2.5 U Taq polymerase with different concentrations of the Ru^{II} complexes. The reaction mixtures were incubated in a thermocycler under the following cycling conditions: 94 °C for 2 min, followed by thirty cycles at 94 °C for 30 s, 58 °C for 30 s and 72 °C for 30 s. The PCR products were then separated by electrophoresis on 12% non-denaturing polyacrylamide gels in 1×TBE and stained with ethidium bromide.

Telomere repeat amplification protocol (TRAP) assay: All of this evidence affirms that the four Ru^{II} complexes have the extraordinary ability to induce and stabilise G-quadruplex formation from telomere DNA. Therefore, further investigation, such as the telomerase inhibition ability, is critical. The TRAP assay (telomeric repeat amplification protocol assay) is a well-developed method used to confirm that the Ru^{II} complexes have the ability to inhibit telomerase in vitro.[24] All of the experiments were performed according to previously published methods that were slightly modified to suit our requirements. NP-40 lysis buffer containing 10 mM Tris-HCl (pH 8.0), 1 mM $MgCl_2$, 1 mM EDTA, 1% (vol/vol) NP-40, 0.25 mM sodium deoxycholate, 10% (vol/vol) glycerol, 150 mM NaCl;,5 mM β-mercaptoethanol and 0.1 mM AEBSF were used to extract whole-cell protein from HeLa cells. In the initial step, the TRAP buffer (20 mM Tris-HCl (pH 8.3), 1.5 mM $MgCl_2$, 63 mM KCl, 0.05% Tween 20 and 1.0 mM EGTA) containing 125 mM dNTPs, 200 ng of TS primer (5′-AATCCGTCGAGCAGAGTT), 100 ng of NT primer (5′-ATCGCTTCTCGGCCTTTT), 100 ng of ACX primer (5′-GCGCGG-CTTACCCTTACCCTTACCCTAACC), 1 μL of 0.01×10^{-18} mol μL^{-1} TSNT oligonucleotide (5′-AATCCGTCGAGCAGAGTTAAAAGGCCGAGAAG-CGAT), 2 U Taq polymerase and 200 cells of protein extract (in 1 μL of NP-40 lysis buffer) were mixed in an RNase-free tube. Secondly, the Ru^{II} complexes were dissolved in DEPC-treated water and prepared as fresh solutions, which were added to the tubes containing the previously described mixture in an appropriate concentration. After all of the components were homogeneously mixed, the samples were incubated at 30 °C for 30 min to allow the extension of the substrate by telomerase. To amplify the extension products by telomerase, the following procedure was performed in a thermal cycler: 95 °C for 5 min to inactivate the telomerase, followed by twenty-four cycles at 95 °C for 30 s, 52 °C for 30 s and 72 °C for 30 s. Afterward, 10 μL of 6×loading dye were added to each TRAP reaction mixture, and 35 μL of the mixture with the loading dye were loaded and resolved on an 8% non-denaturing acrylamide gel in 1×TBE (100 min, 25 V cm^{-1}) that was stained with ethidium bromide.[65]

Short-term cell viability: Short-term cytotoxicity of the complexes was determined by a standard MTT assay. Because living cells transform MTT to a purple formazan dye, the yield of formazan transformed by the cells exposed to the proper concentration of complexes was used to measure cytotoxicity.[66,67] First, cells were grown in an RPMI 1640 medium containing FBS (10%), penicillin (100 μg mL^{-1}) and streptomycin (100 μg mL^{-1}). The cells were incubated at 37 °C in a humidified incubator with 5% CO_2 to the exponential growth phase. Then, the cells were diluted, seeded in 96-well microassay culture plates (1×10^4 cells per well) and incubated under the same conditions previously used. After being incubated for 24 h, the cells were treated with various concentrations of the complexes. The tested compounds were subsequently dissolved in sterile water and diluted with RPMI 1640 to the required concentrations. The medium and drug-free control samples were prepared simultaneously. After the cells were incubated for another 48 h, a stock MTT dye solution (20 μL, 5 mg mL^{-1}) was added to each well. After further incubation (4 h), all of the solutions in the wells were discarded and 150 μL of DMSO were added to dissolve the MTT formazan. The plate was analysed on a microplate spectrophotometer at a wavelength of $\lambda = 570$ nm. The absorption data were plotted on a logarithmic graph of the percent viability read-

ing of the control versus the concentration. IC_{50} is the concentration at which 50% of the cells were viable relative to the control. Each experiment was repeated a minimum of three times to obtain mean values. The HeLa (cervical) cell line was the subject of this study.

Long-term proliferation experiments: The traditional method to detect long-term cell proliferation is to seed the cells onto a 96-well plate and then culture, digest, dilute and reseed the cells for more than ten days. After this process, the cells remaining in the wells are stained with a SA-β-Gal staining kit for detection of the expression of SA-β-Gal to determine the cell senescence and apoptosis.[68] Because this approach represents an end-point analytical method, we could not monitor the cell growth conditions while the experiment was in progress.[54] To overcome this shortcoming, we used the xCELLigence system in our experiment. The xCELLigence system offers a dynamic, real-time, label-free and non-invasive analysis of a variety of cellular events. It can monitor cellular events in real time without the incorporation of labels or any other substances that may inhibit cell proliferation over a long period. The system measures the electrical impedance switch as a dimensionless parameter, termed the cell index (CI), across interdigitated micro-electrodes on the bottom of tissue culture E-plates. Under the same physiological conditions, the CI values are greater when more cells are attached to the electrodes. Thus, the CI value can represent the cell status, including the quantitative number of cells present in a well. Herein, we designed a new method to exploit the advantages of the xCELLigence system to their full potential.[21] Long-term proliferation experiments were performed according to the following procedure: HeLa cells (5.0×10^3 cells) were seeded in a 16-well E-plate. A subcytotoxic concentration (2.5 μM) of a complex was added to the experimental wells, whereas an equivalent volume of 0.1% DMSO was added to the control wells, Each well contained three parallel controls. Every three days, the cells in the drug-exposed and control wells were collected, diluted tenfold and reseeded into the same wells. This process enhances the different statuses between the control cells and the drug-exposed cells, including the cell number and shape. This experiment was continued for approximately ten days.

Molecular modelling: Geometry optimisations for all of the ligands were performed by the density functional B3LYP method with a mixed basis set (SDD was used for Ru and 6-31G* was used for the other atoms) by using the Gaussian 03 program.[69] Crystal structures of parallel quadruplexes from the human telomeric DNA sequence $d(AG_3[T_2AG_3]_3)$ with K^+ and Na^+ were extracted from the protein data bank (PDB ID 1KF1 and 143D, respectively). The Amber FF99 force field was applied to the proteins after the solvent/ions were removed and hydrogen atoms were added. Because the space between two G-quadruplets in PDB 143D was too narrow, one of the phosphate backbones at the 5′-AG step was broken to enlarge the space to hold these ligands, and then reconnected following by 1000 steps steepest descent minimisation.[70] The Surflex-Dock (SFXC) module in SYBYL 7.3 (Tripos, Inc.) was used to perform docking processes. In the docking analysis, predock and post-dock minimisations were not performed and the ring flexibility was considered. Other parameters included 100 additional starting conformations per molecule and an expanded search grid of 5.00 Å. To further elucidate the interactions between the dinuclear ruthenium(II) complexes and the G-quadruplexes, the best-scored docking conformations were introduced as the starting structures in molecular dynamics (MD). Force field Amber FF99SB was used for the DNA, whereas the GAFF force field was applied for the ligands. The restrained electrostatic potential (RESP) charges were calculated by the RESP module in AMBER[57] and were set for the four complexes. After being neutrally charged by their own ions in solution, the combined systems were solvated into an octahedral box of TIP3P water, resulting in a 12 Å separation of the complexes. The normal state of 300 K and 1 atm were set in the MD simulations. The 8 Å distance of the non-bonded cut-off value was adopted to avoid interactions from atoms in an adjacent periodic box or from long-range electrostatic forces. The MD calculations proceeded with the following steps: 200 steps of the steepest descent minimisation, 20 ps MD simulation of hydrogen atoms with constant pressure, 60 ps MD equilibration with constant pressure and 4.2 ns of MD equilibrations. Fifty snapshots were extracted from the last 0.2 ns of the trajectories (at 4 ps intervals) in each binding system. Their binding free energy values, ΔG_{bind}, were obtained by performing calculations of molecular mechanics/generalised Born surface area (MM/GBSA).[71] The ΔG_{bind} value is given by summing the electrostatic energy values (ΔG_{ele}), the non-electrostatic energy values ($\Delta G_{non\text{-}ele}$) and the entropy component ($T\Delta S$). In a solvent system, ΔG_{ele} can be split into the electrostatic energy in the gas phase and the electrostatic contribution to the solvation free energy, whereas $\Delta G_{non\text{-}ele}$ consists of the van der Waals (ΔE_{vdW}) energy and the nonpolar contributions to the solvation free energy. The entropy contributions were not considered in this study because of the structural similarity of the ruthenium complexes. All of the calculations of MD and MM/GBSA, as well as their preparations, were performed by using Amber10.[47] Moreover, the central cations were not included in the MD modelling because no Na^+ ions were available in the crystal structure of its assembling parallel quadruplexes.

Acknowledgements

This work was supported by the 973 program (2014CB845604), the National Science Foundation of China (Nos. 21172273, 21171177 and 91122010), the Program for Changjiang Scholars and Innovative Research Team in University of China (No. IRT1298) and the Research Fund for the Doctoral Program of Higher Education (20110171110013). L.X. thanks the support of the National Science Foundation of China (21301034) and the National Science Foundation of Guangdong Province (S2013040014083).

Keywords: conformation analysis · DNA · G-quadruplexes · ruthenium · telomeres

[1] G. N. Parkinson, M. P. H. Lee, S. Neidle, *Nature* **2002**, *417*, 876–880.
[2] J. T. Davis, *Angew. Chem. Int. Ed.* **2004**, *43*, 668–698; *Angew. Chem.* **2004**, *116*, 684–716.
[3] J. L. Huppert, *Chem. Soc. Rev.* **2008**, *37*, 1375–1384.
[4] E. Henderson, C. C. Hardin, S. K. Walk, I. Tinoco, Jr., E. H. Blackburn, *Cell* **1987**, *51*, 899–908.
[5] D. Sen, W. Gilbert, *Nature* **1988**, *334*, 364–366.
[6] T. S. Dexheimer, D. Sun, L. H. Hurley, *J. Am. Chem. Soc.* **2006**, *128*, 5404–5415.
[7] S. Rankin, A. P. Reszka, J. Huppert, M. Zloh, G. N. Parkinson, A. K. Todd, S. Ladame, S. Balasubramanian, S. Neidle, *J. Am. Chem. Soc.* **2005**, *127*, 10584–10589.
[8] T. Simonsson, P. Pecinka, M. Kubista, *Nucleic Acids Res.* **1998**, *26*, 1167–1172.
[9] A. De Cian, L. Lacroix, C. Douarre, N. Temime-Smaali, C. Trentesaux, J. F. Riou, J. L. Mergny, *Biochimie* **2008**, *90*, 131–155.
[10] P. Alberti, L. Lacroix, L. Guittat, C. Hélène, J.-L. Mergny, *Mini-Rev. Med. Chem.* **2003**, *3*, 23–36.

[11] S. Balasubramanian, L. H. Hurley, S. Neidle, *Nat. Rev. Drug Discovery* **2011**, *10*, 261 – 275.
[12] S. Neidle, *Curr. Opin. Struct. Biol.* **2009**, *19*, 239 – 250.
[13] D. Yang, K. Okamoto, *Future Med. Chem.* **2010**, *2*, 619 – 646.
[14] J. H. Tan, L. Q. Gu„ J. Y. Wu, *Mini-Rev. Med. Chem.* **2008**, *8*, 1163 – 1178.
[15] G. N. Parkinson, F. Cuenca, S. Neidle, *J. Mol. Biol.* **2008**, *381*, 1145 – 1156.
[16] K. N. Luu, A. T. Phan, V. Kuryavyi, L. Lacroix, D. J. Patel, *J. Am. Chem. Soc.* **2006**, *128*, 9963 – 9970.
[17] T. Wilson, P. J. Costa, V. Felix, M. P. Williamson, J. A. Thomas, *J. Med. Chem.* **2013**, *56*, 8674 – 8683.
[18] T. Li, E. Wang, S. Dong, *Anal. Chem.* **2010**, *82*, 7576 – 7580.
[19] F. Hamon, E. Largy, A. Guedin-Beaurepaire, M. Rouchon-Dagois, A. Sidibe, D. Monchaud, J. Mergny, J. Riou, C. Nguyen, M. Teulade-Fichou, *Angew. Chem. Int. Ed.* **2011**, *50*, 8745 – 8749; *Angew. Chem.* **2011**, *123*, 8904 – 8908.
[20] R. Hansel, F. Lohr, S. Foldynova-Trantirkova, E. Bamberg, L. Trantirek, V. Dotsch, *Nucleic Acids Res.* **2011**, *39*, 5768 – 5775.
[21] C. Rajput, R. Rutkaite, L. Swanson, I. Haq, J. A. Thomas, *Chem. Eur. J.* **2006**, *12*, 4611 – 4619.
[22] D. Sun, Y. Liu, D. Liu, R. Zhang, X. Yang, J. Liu, *Chem. Eur. J.* **2012**, *18*, 4285 – 4295.
[23] X. Chen, J. H. Wu, Y. W. Lai, R. Zhao, H. Chao, L. N. Ji, *Dalton Trans.* **2013**, *42*, 4386 – 4397.
[24] D. D. Sun, R. Zhang, F. Yuan, D. Liu, Y. H. Zhou, J. Liu, *Dalton Trans.* **2012**, *41*, 1734 – 1741.
[25] S. Shi, J. Liu, T. M. Yao, X. T. Geng, L. F. Jiang, Q. Y. Yang, L. Cheng, L. N. Ji, *Inorg. Chem.* **2008**, *47*, 2910 – 2912.
[26] S. Shi, J. Zhao, X. Gao, C. Y. Lv, L. Yang, J. Hao, H. L. Huang, J. L. Yao, W. L. Sun, T. M. Yao, L. N. Ji, *Dalton Trans.* **2012**, *41*, 5789 – 5793.
[27] J. L. Yao, X. Gao, W. L. Sun, X. Z. Fan, S. Shi, T. M. Yao, *Inorg. Chem.* **2012**, *51*, 12591 – 12593.
[28] T. Wilson, M. P. Williamson, J. A. Thomas, *Org. Biomol. Chem.* **2010**, *8*, 2617 – 2621.
[29] L. Xu, D. Zhang, J. Huang, M. G. Deng, M. Zhang, X. Zhou, *Chem. Commun.* **2010**, *46*, 743 – 745.
[30] G. A. L. Bare, B. Liu„ J. C. Sherman, *J. Am. Chem. Soc.* **2013**, *135*, 11985 – 11989.
[31] W. J. Chung, B. Heddi, M. Tera, K. Iida, K. Nagasawa, A. T. Phan, *J. Am. Chem. Soc.* **2013**, *135*, 13495 – 13501.
[32] X. X. Wang, C. X. Zhou, J. W. Yan, J. Q. Hou, S. B. Chen, T. M. Ou, L. Q. Gu, Z. S. Huang, J. H. Tan, *ACS Med. Chem. Lett.* **2013**, *4*, 909 – 914.
[33] M. Franceschin, *Eur. J. Org. Chem.* **2009**, 2225 – 2238.
[34] N. Ranjan, E. Davis, L. Xue, D. P. Arya, *Chem. Commun.* **2013**, *49*, 5796 – 5798.
[35] T. M. Ou, Y. J. Lu, J. H. Tan, Z. S. Huang, K. Y. Wong, L. Q. Gu, *ChemMedChem* **2008**, *3*, 690 – 713.
[36] D. L. Ma, C. M. Che, S. C. Yan, *J. Am. Chem. Soc.* **2009**, *131*, 1835 – 1846.
[37] S. Bianco, C. Musetti, A. Waldeck, S. Sparapani, J. D. Seitz, A. P. Krapcho, M. Palumbo, C. Sissi, *Dalton Trans.* **2010**, *39*, 5833 – 5841.
[38] K. Suntharalingam, O. Mendoza, A. A. Duarte, D. J. Mann, R. Vilar, *Metallomics* **2013**, *5*, 514 – 523.
[39] K. Suntharalingam, A. J. P. White, R. Vilar, *Inorg. Chem.* **2010**, *49*, 8371 – 8380.
[40] S. N. Georgiades, N. H. Abd Karim, K. Suntharalingam, R. Vilar, *Angew. Chem. Int. Ed.* **2010**, *49*, 4020 – 4034; *Angew. Chem.* **2010**, *122*, 4114 – 4128.
[41] J. Zhou, G. Yuan, *Chem. Eur. J.* **2007**, *13*, 5018 – 5023.
[42] D. P. N. Goncalves, S. Ladame, S. Balasubramanian, J. K. M. Sanders, *Org. Biomol. Chem.* **2006**, *4*, 3337 – 3342.
[43] R. Giraldo, M. Suzuki, L. Chapman, D. Rhodes, *Proc. Natl. Acad. Sci. USA* **1994**, *91*, 7658 – 7662.
[44] V. Dapić, V. Abdomerović, R. Marrington, J. Peberdy, A. Rodger, J. O. Trent, P. J. Bates, *Nucleic Acids Res.* **2003**, *31*, 2097 – 2107.
[45] E. M. Rezler, J. Seenisamy, S. Bashyam, M. Y. Kim, E. White, W. D. Wilson, L. H. Hurley, *J. Am. Chem. Soc.* **2005**, *127*, 9439 – 9447.
[46] Y. Xue, Z. Y. Kan, Q. Wang, Y. Yao, J. Liu, Y. H. Hao, Z. Tan, *J. Am. Chem. Soc.* **2007**, *129*, 11185 – 11191.
[47] AMBER 10, D. A. Case, T. A. Darden, T. E. Cheatham III, C. L. Simmerling, J. Wang, R. E. Duke, R. Luo, M. Crowley, R. C. Walker, W. Zhang, K. M. Merz, B. Wang, S. Hayik, A. Roitberg, G. Seabra, I. Kolossváry, K. F. Wong, F. Paesani, J. Vanicek, X. Wu, S. R. Brozell, T. Steinbrecher, H. Gohlke, L. Yang, C. Tan, J. Mongan, V. Hornak, G. Cui, D. H. Mathews, M. G. Seetin, C. Sagui, V. Babin, P. A. Kollman, University of California, San Francisco, **2008**.
[48] X. H. Zheng, Y. F. Zhong, C. P. Tan, L. N. Ji, Z. W. Mao, *Dalton Trans.* **2012**, *41*, 11807 – 11812.
[49] G. W. Collie, R. Promontorio, S. M. Hampel, M. Micco, S. Neidle, G. N. Parkinson, *J. Am. Chem. Soc.* **2012**, *134*, 2723 – 2731.
[50] C. Y. Chen, Q. Wang, J. Q. Liu, Y. H. Hao, Z. Tan, *J. Am. Chem. Soc.* **2011**, *133*, 15036 – 15044.
[51] V. Hanusova, V. Kralova, L. Schroterova, L. Trilecova, A. Pakostova, L. Skalova, *Xenobiotica* **2010**, *40*, 681 – 690.
[52] Y. Chen, K. G. Qu, C. Q. Zhao, L. Wu, J. S. Ren, J. S. Wang, X. G. Qu, *Nat. Commun.* **2012**, *3*, 1074.
[53] Z. H. Siddik, *Oncogene* **2003**, *22*, 7265 – 7279.
[54] W. B. Wu, S. H. Chen, J. Q. Hou, J. H. Tan, T. M. Ou, S. L. Huang, D. Li, L. Q. Gu, Z. S. Huang, *Org. Biomol. Chem.* **2011**, *9*, 2975 – 2986.
[55] E. S. Baker, J. T. Lee, J. L. Sessler, M. T. Bowers, *J. Am. Chem. Soc.* **2006**, *128*, 2641 – 2648.
[56] F. R. Liu, K. Z. Wang, G. Y. Bai, Y. A. Zhang, L. H. Gao, *Inorg. Chem.* **2004**, *43*, 1799 – 1806.
[57] H. Chao, Y. X. Yuan, F. Zhou, L. N. Ji, *Transit. Met. Chem.* **2006**, *31*, 465 – 469.
[58] W. Paw, R. Eisenberg, *Inorg. Chem.* **1997**, *36*, 2287 – 2293.
[59] J. Bolger, A. Gourdon, E. Ishow, J. P. Launay, *Inorg. Chem.* **1996**, *35*, 2937 – 2944.
[60] L. J. Chen, G. D. Qian, Y. J. Cui, X. F. Jin, Z. Y. Wang, M. Q. Wang, *J. Phys. Chem. B* **2006**, *110*, 19176 – 19182.
[61] A. D. Moorhouse, A. M. Santos, M. Gunaratnam, M. Moore, S. Neidle, J. E. Moses, *J. Am. Chem. Soc.* **2006**, *128*, 15972 – 15973.
[62] A. De Cian, E. Delemos, J. L. Mergny, M. P. Teulade-Fichou, D. Monchaud, *J. Am. Chem. Soc.* **2007**, *129*, 1856 – 1857.
[63] P. Job, *Ann. Chim.* **1928**, *9*, 113 – 203.
[64] T. Lemarteleur, D. Gomez, R. Paterski, E. Mandine, P. Maillet, J. F. Riou, *Biochem. Biophys. Res. Commun.* **2004**, *323*, 802 – 808.
[65] J. Reed, M. Gunaratnam, M. Beltran, A. P. Reszka, R. Vilar, S. Neidle, *Anal. Biochem.* **2008**, *380*, 99 – 105.
[66] S. Kemp, N. J. Wheate, D. P. Buck, M. Nikac, J. G. Collins, J. R. Aldrich-Wright, *J. Inorg. Biochem.* **2007**, *101*, 1049 – 1058.
[67] J. Ai, W. Guo, B. Li, T. Li, D. Li, E. Wang, *Talanta* **2012**, *88*, 450 – 455.
[68] J. F. Riou, L. Guittat, P. Mailliet, A. Laoui, E. Renou, O. Petitgenet, F. Megnin-Chanet, C. Helene, J. L. Mergny, *Proc. Natl. Acad. Sci. USA* **2002**, *99*, 2672 – 2677.
[69] Gaussian 03, Revision D.01, M. J. Frisch, G. W. Trucks, H. B. Schlegel, G. E. Scuseria, M. A. Robb, J. R. Cheeseman, J. A. Montgomery, Jr., T. Vreven, K. N. Kudin, J. C. Burant, J. M. Millam, S. S. Iyengar, J. Tomasi, V. Barone, B. Mennucci, M. Cossi, G. Scalmani, N. Rega, G. A. Petersson, H. Nakatsuji, M. Hada, M. Ehara, K. Toyota, R. Fukuda, J. Hasegawa, M. Ishida, T. Nakajima, Y. Honda, O. Kitao, H. Nakai, M. Klene, X. Li, J. E. Knox, H. P. Hratchian, J. B. Cross, V. Bakken, C. Adamo, J. Jaramillo, R. Gomperts, R. E. Stratmann, O. Yazyev, A. J. Austin, R. Cammi, C. Pomelli, J. W. Ochterski, P. Y. Ayala, K. Morokuma, G. A. Voth, P. Salvador, J. J. Dannenberg, V. G. Zakrzewski, S. Dapprich, A. D. Daniels, M. C. Strain, O. Farkas, D. K. Malick, A. D. Rabuck, K. Raghavachari, J. B. Foresman, J. V. Ortiz, Q. Cui, A. G. Baboul, S. Clifford, J. Cioslowski, B. B. Stefanov, G. Liu, A. Liashenko, P. Piskorz, I. Komaromi, R. L. Martin, D. J. Fox, T. Keith, M. A. Al-Laham, C. Y. Peng, A. Nanayakkara, M. Challacombe, P. M. W. Gill, B. Johnson, W. Chen, M. W. Wong, C. Gonzalez, J. A. Pople, Gaussian, Inc., Wallingford CT, **2004**.
[70] M. Read, R. J. Harrison, B. Romagnoli, F. A. Tanious, S. H. Gowan, A. P. Reszka, W. D. Wilson, L. R. Kelland, S. Neidle, *Proc. Natl. Acad. Sci. USA* **2001**, *98*, 4844 – 4849.
[71] J. Srinivasan, T. E. Cheatham III, P. Cieplak, P. A. Kollman, D. A. Case, *J. Am. Chem. Soc.* **1998**, *120*, 9401 – 9409.

Received: November 6, 2014
Published online on ■■ ■■, 0000

FULL PAPER

G-Quadruplexes

*L. Xu, X. Chen, J. Wu, J. Wang, L. Ji, H. Chao**

■■ – ■■

Dinuclear Ruthenium(II) Complexes That Induce and Stabilise G-Quadruplex DNA

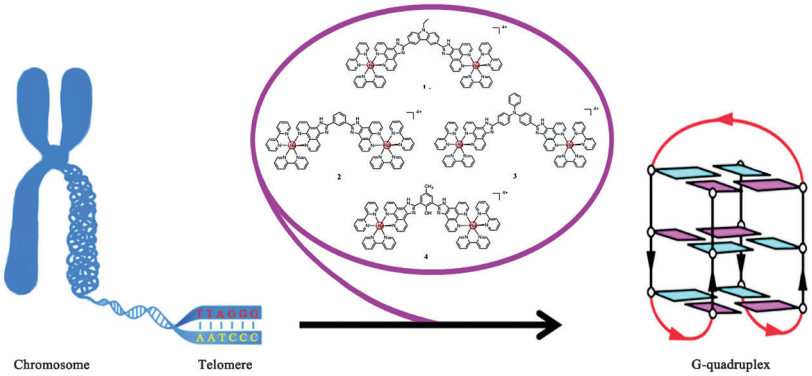

Being blocked by Ru: A series of dinuclear ruthenium(II) complexes (see figure) were found to promote high stabilisation of the G-quadruplexes of human telomeric DNA and exhibited a high telomerase inhibiting activity.